rotation on $La(L)(CF_3SO_3)_2^+$], Table XX [polyhedral angles for $La(L)(CF_3SO_3)_2^+$], Figure 4 [stereoview of the hydrogen bonding around $[La(en)_4(CF_3SO_3)]^{2+}$], Figure 5 [stereoview of the unit cell packing diagram for $La(en)_4(CH_3CN)(CF_3SO_3)_3$], Figure 9 [stereoview of the hydrogen bonding around $[La(L)(CF_3SO_3)_2]^+$], Figure 10 [stereoview of the unit cell packing diagram for $La(L)(CH_3CN)(CF_3SO_3)_3$], Figure 14 [stereoview of the hydrogen bonding around $[Yb(L)(CF_3SO_3)]^{2+}$], and Figure 15 [stereoview of the unit cell packing diagram for $Yb(L)(CH_3CN)(CF_3SO_3)_3$] (156 pages). Ordering information is given on any current masthead page.

Contribution from the Department of Chemistry,
The University of Michigan, Ann Arbor, Michigan 48109

Tertiary Alkylphosphine Adducts of $Mo_2(O_2CCF_3)_4$ (Mo–Mo)[1]

D. J. SANTURE and A. P. SATTELBERGER*[2]

Received September 5, 1984

$Mo_2(O_2CCF_3)_4$ reacts with 2 equiv of PR_3 (R = Me, Et, *n*-Bu) in toluene to give adducts of stoichiometry $Mo_2(O_2CCF_3)_4 \cdot 2PR_3$. These complexes have been characterized by solid-state infrared spectroscopy and variable-temperature ^{19}F and $^{31}P\{^1H\}$ NMR. A *single* isomer, with equatorially bound phosphines, is observed in solution at temperatures below ca. −40 °C in each case. Previous work on the PMe_3 and PEt_3 adducts suggested that there were two or more equatorial isomers present in solution at low temperature. The discrepancy between the two studies can be traced to the purity of $Mo_2(O_2CCF_3)_4$, which is usually prepared by metathesis of $Mo_2(O_2CCH_3)_4$ in refluxing trifluoroacetic acid. In our hands, this procedure gives a product contaminated with $Mo_2(O_2CCF_3)_3(O_2CCH_3)$. X-ray structural studies on $Mo_2(O_2CCF_3)_4 \cdot 2PBu_3$ show that this complex has a C_{2h} core, which is presumably maintained in solution. The Mo–Mo and Mo–P bond lengths are 2.105 (1) and 2.542 (2) Å, respectively. The differences in solution behavior between homologous $M_2(O_2CCF_3)_4 \cdot 2PR_3$ complexes (M = Mo, W) are discussed and correlated with M–P bond strengths. Phosphine-exchange reactions are used to generate the mixed-phosphine equatorial adducts $M_2(O_2CCF_3)_4 \cdot PEt_3 \cdot PBu_3$ (M = Mo, W) in solution. The electronic absorption spectra of $M_2(O_2CCF_3)_4 \cdot 2PMe_3$ (M = Mo, W) are reported and the $\delta \rightarrow \delta^*$, $^1A_g \rightarrow {}^1B_u$ transitions are assigned and discussed. Crystal data (at −125 °C) for $Mo_2(O_2CCF_3)_4 \cdot 2PBu_3$ are as follows: monoclinic space group $I2/a$, a = 19.390 (10) Å, b = 10.414 (4) Å, c = 21.790 (11) Å, β = 94.64 (4)°, V = 4385.58 Å^3, Z = 4, d_{calcd} = 1.586 g cm^{-3}.

Introduction

There are several reports in the literature on the reactions of tetrakis(trifluoroacetato)dimolybdenum(II), $Mo_2(TFA)_4$, with tertiary phosphines,[3-5] and two general classes of $Mo_2(TFA)_4 \cdot 2PR_3$ complexes have been isolated and characterized by IR, NMR, and X-ray crystallography. The class I complexes, obtained with bulky phosphines, are simple axial adducts (A). Two members

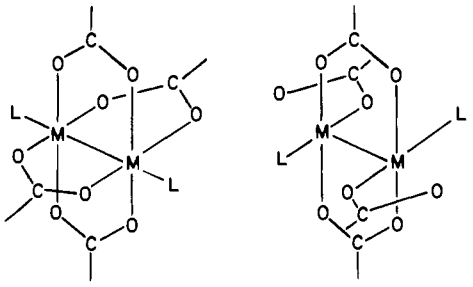

A B

of this class have been examined crystallographically,[4,5] and both have rather long Mo–P bonds (>2.96 Å), implying only a weak interaction. Not surprisingly, these adducts are extensively dissociated in solution.[3]

The reactions of $Mo_2(TFA)_4$ with small, basic tertiary phosphines, e.g., triethylphosphine, provide class II complexes. In these, one equatorially bound oxygen on each of two trifluoroacetate ligands is displaced by a phosphine. Six geometrical isomers are possible for an $Mo_2(TFA)_4 \cdot 2PR_3$ dimer[3] containing only one pair of bidentate $CF_3CO_2^-$ ligands, and one of these (the C_{2h} isomer) is shown (B). Two members of this class have also been studied by X-ray crystallography.[4] A C_{2h} core structure was found for both, and the Mo–P bonds (2.51–2.53 Å) were appreciably shorter than those found in the class I structures. The solution behavior of several class II compounds has been examined by variable-temperature $^{31}P\{^1H\}$ and ^{19}F NMR spectroscopy and was not amenable to any simple interpretation.[3] At least two equatorial isomers were observed in $CDCl_3$ solutions of the class II complexes, and their stereochemistry could not be determined by spectroscopic techniques.[3]

In a recent paper,[6] we described the syntheses and physicochemical properties of several class II phosphine adducts of tetrakis(trifluoroacetato)ditungsten(II). We found that a single equatorial isomer was present in solutions of $W_2(TFA)_4 \cdot 2PR_3$ (R = Me, Et, *n*-Bu), as judged by variable-temperature ^{19}F and $^{31}P\{^1H\}$ NMR spectroscopy. Furthermore, a comparison of the solid-state and solution infrared spectra, coupled with the crystal structure of $W_2(TFA)_4 \cdot 2PBu_3$, a C_{2h} isomer, led us to conclude that the solution and solid-state structures of each complex were identical. We then speculated that the differences in solution behavior between homologous $M_2(TFA)_4 \cdot 2PR_3$ complexes were a reflection of the differences in M–P bond strengths, i.e., W–P > Mo–P. However, it was not clear what connection, if any, there was between weak Mo–P bonds and the observation of multiple equatorial isomers in solution. As a consequence, we decided to reinvestigate the solution behavior of several class II phosphine adducts of $Mo_2(TFA)_4$. Our results, which differ from those reported earlier,[3] are described herein together with the X-ray structure of $Mo_2(TFA)_4 \cdot 2PBu_3$.

Results and Discussion

Synthesis of $Mo_2(TFA)_4$. The $Mo_2(TFA)_4$ used in our studies was prepared by a route that is quite different than the one described in the literature.[7] Polymeric molybdenum trichloride was reduced in THF with sodium amalgam in the presence of 2 equiv of sodium trifluoroacetate to provide dark yellow-brown solutions containing $Mo_2(TFA)_4$ (reaction 1). After filtration,

$$MoCl_3 + Na/Hg + 2NaO_2CCF_3 \xrightarrow{THF} 0.5Mo_2(O_2CCF_3)_4 + 3NaCl \quad (1)$$

solvent removal, and sublimation (100 °C, 10^{-5} torr) of the brown

(1) Metal-Metal Bonded Complexes of the Early Transition Metals. 10. Part 9: Santure, D. J.; Huffman, J. C.; Sattelberger, A. P. *Inorg. Chem.* **1985**, *24*, 371.
(2) Present address: Los Alamos National Laboratory, INC-4, Mail Stop C345, Los Alamos, NM 87545.
(3) Girolami, G. S.; Mainz, V. V.; Andersen, R. A. *Inorg. Chem.* **1980**, *19*, 805.
(4) Cotton, F. A.; Lay, D. G. *Inorg. Chem.* **1981**, *20*, 935.
(5) Girolami, G. S.; Andersen, R. A. *Inorg. Chem.* **1982**, *21*, 1318.
(6) Santure, D. J.; Huffman, J. C.; Sattelberger, A. P. *Inorg. Chem.* **1984**, *23*, 938.
(7) Cotton, F. A.; Norman, J. G., Jr. *J. Coord. Chem.* **1971**, *1*, 161.

0020-1669/85/1324-3477$01.50/0

residue, pure (MS, ^1H NMR, ^{19}F NMR), bright yellow $Mo_2(TFA)_4$ was isolated in ca. 20% yield, based on $[MoCl_3]_x$. This procedure is a modification of that used to prepare $W_2(TFA)_4$ from $[WCl_4]_x$.[8]

Synthesis and Characterization of $Mo_2(TFA)_4 \cdot 2PR_3$ Compounds. Toluene solutions of $Mo_2(TFA)_4$ react readily with PMe_3, PEt_3, and PBu_3 to yield orange complexes **1a–c**, according to reaction 2. This procedure is identical with that used in the preparation

$$Mo_2(TFA)_4 + 2PR_3 \xrightarrow{PhCH_3} Mo_2(TFA)_4 \cdot 2PR_3 \quad (2)$$

1a, R = Me
1b, R = Et
1c, R = *n*-Bu

of the $W_2(TFA)_4 \cdot 2PR_3$ (R = Me, Et, *n*-Bu) compounds.[6] All of these molybdenum complexes are moderately air sensitive in the solid state, decomposing within 1–2 h. Complexes **1b** and **1c** are soluble in toluene, THF, and chloroform and insoluble in hexane. **1a**, like its tungsten homologue,[6] is appreciably soluble only in THF. Solutions of the adducts are considerably more air sensitive than the solids. All of the adducts are temperature sensitive (**1c** > **1b** > **1a**) and decompose to $Mo_2(TFA)_4$ and free phosphine when heated in vacuo. Unlike $W_2(TFA)_4 \cdot 2PMe_3$,[6] which shows a strong parent ion (P^+) in its electron impact mass spectrum, **1a** shows only $P - 2PMe_3^+$, i.e., only the $Mo_2(TFA)_4$ cation. We take this as evidence that the phosphine ligands in the $Mo_2(TFA)_4 \cdot 2PR_3$ compounds are less tightly bound than in their tungsten homologues (vide infra).

The solid-state infrared spectra (Nujol mulls) of each of the molybdenum adducts show two well-resolved antisymmetric C–O stretching modes, one in the region characteristic of monodentate $CF_3CO_2^-$ coordination[9] (ca. 1670 cm^{-1}) and one in the region characteristic of bidentate $CF_3CO_2^-$ coordination[9] (ca. 1580 cm^{-1}). For comparison, the parent complex, $Mo_2(TFA)_4$, with four bidentate, bridging carboxylate ligands, has its antisymmetric C–O stretching mode at 1595 cm^{-1}.

The ^{19}F and $^{31}P\{^1H\}$ NMR spectra of **1b** and **1c** have been recorded as a function of temperature in toluene-d_8 and chloroform-*d*. **1a** has minimal solubility in these solvents, so its spectra were recorded in THF. The spectra are all qualitatively similar, so we need only discuss one set of them. The room-temperature 36.2-MHz $^{31}P\{^1H\}$ NMR spectrum of **1c**, in toluene-d_8, shows a single broad ($\Delta\nu_{1/2}$ = 120 Hz) resonance at δ +4.0. This peak sharpens and shifts downfield as the temperature is lowered. At −70 °C, the line width is 12 Hz and the chemical shift is δ +11.0 (see Figure 1). The temperature dependence of the $^{31}P\{^1H\}$ NMR spectrum was completely reversible. Similar results were obtained in $CDCl_3$; i.e., *only one* phosphorus resonance was observed from +25 to −60 °C.

The room-temperature 84.3-MHz ^{19}F NMR spectrum of $Mo_2(TFA)_4 \cdot 2PBu_3$, in toluene-d_8, shows two overlapping broad resonances ($\Delta\nu_{1/2}$ = 70 Hz) at ca. δ −72 and −75. These sharpen and separate as the temperature is lowered. At −70 °C, two area 1 singlets ($\Delta\nu_{1/2}$ = 8 Hz) are observed at δ −71.3 and −74.6 (Figure 1). These chemical shifts are indicative of bidentate[10] and monodentate[11] $CF_3CO_2^-$ coordination, respectively. The ^{19}F NMR spectrum of $Mo_2(TFA)_4$ (toluene-d_8, 25 °C) shows a single "bidentate" resonance at δ −72.0. The temperature dependence of the ^{19}F NMR spectrum of **1c** was reversible. Similar results were obtained in $CDCl_3$.

The NMR data on **1a–c** indicate that there is only one equatorial isomer present in solution at low temperature and that this isomer is in equilibrium with $Mo_2(TFA)_4$ and free phosphine near room temperature (reaction 3). By analogy with our results on

$$Mo_2(TFA)_4 \cdot 2PR_3 \rightleftharpoons Mo_2(TFA)_4 + 2PR_3 \quad (3)$$

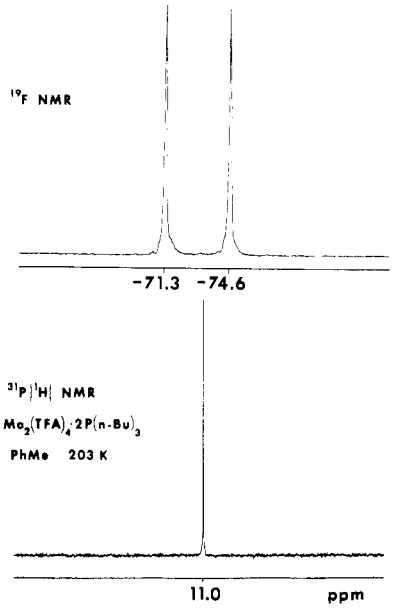

Figure 1. 84.26-MHz ^{19}F NMR (top) and 36.20-MHz $^{31}P\{^1H\}$ NMR (bottom) spectra of $Mo_2(TFA)_4 \cdot 2PBu_3$ recorded in toluene-d_8 at −70 °C.

the corresponding, and more stable, $W_2(TFA)_4 \cdot 2PR_3$ complexes,[6] we suggest that the equatorial isomer present in these solutions is the one with a C_{2h} core.

It is not entirely clear why our spectroscopic results on $Mo_2(TFA)_4 \cdot 2PMe_3$ and $Mo_2(TFA)_4 \cdot 2PEt_3$ differ from those reported in the literature,[3] but we think it can be traced to the preparation of $Mo_2(TFA)_4$. We have found that a *fivefold scale-up* of the original synthesis[7] of this dimer (reaction 4) provides a crude

$$Mo_2(O_2CCH_3)_4 + \text{excess } HO_2CCF_3 \xrightarrow[\Delta]{(CF_3CO)_2O} Mo_2(O_2CCF_3)_4 + 4HO_2CCH_3 \quad (4)$$

product that is contaminated by appreciable amounts (up to ~40%) of the mixed-ligand species $Mo_2(O_2CCF_3)_3(O_2CCH_3)$.[12] Unless sufficient care is exercised during the sublimation of this product, pure $Mo_2(TFA)_4$ is not obtained. Phosphine adducts prepared with "impure" $Mo_2(TFA)_4$ show multiple, low-temperature ^{31}P and ^{19}F NMR resonances, which might easily be mistaken for different equatorial isomers of "pure" $Mo_2(TFA)_4$.

Now that we have established the presence of only one equatorial isomer in solutions of $Mo_2(TFA)_4 \cdot 2PR_3$ *or* $W_2(TFA)_4 \cdot 2PR_3$ (R = alkyl), the next question we want to address is why there is a difference in the solution behavior of homologous molybdenum and tungsten adducts. The mass spectral results (vide supra) suggest that equatorial Mo–P bonds are weaker than their tungsten counterparts. In the next section, we provide structural data that confirm this hypothesis.

Solid-State Structure of $Mo_2(TFA)_4 \cdot 2PBu_3$. Crystal data for **1c** are provided in Table I. Final atomic coordinates are given in Table II. Interatomic distances and angles are listed in Table III (supplementary material). In the space group *I*2/*a* (a nonstandard setting of the monoclinic space group *C*2/*c*) with *Z* = 4, crystallographic inversion symmetry is imposed on **1c**. An ORTEP drawing of the molecule is shown in Figure 2. We have deleted the ordered *n*-butyl groups on the phosphines so that the C_{2h} core of the dimer can be seen clearly.

Not unexpectedly, the structure of **1c** is qualitatively similar to that of $W_2(TFA)_4 \cdot 2PBu_3$.[6] Some key bond distances and angles for the two structures are listed in Table IV. Aside from the increase in M–M bond length (Mo → W), the only substantive difference between **1c** and its tungsten homologue is the M–P bond lengths, i.e., 2.542 (2) Å in **1c** and 2.489 (3) Å in $W_2(TFA)_4 \cdot 2PBu_3$. Since the covalent radii of molybdenum and tungsten are

(8) Santure, D. J.; McLaughlin, K. W.; Huffman, J. C.; Sattelberger, A. P. *Inorg. Chem.* **1983**, *22*, 1877.
(9) Garner, C. D.; Hughes, B. *Adv. Inorg. Chem. Radiochem.* **1975**, *17*, 1.
(10) Teremoto, K.; Sasaki, Y.; Nigita, K.; Iwaizumi, M.; Soito, K. *Bull. Chem. Soc. Jpn.* **1979**, *52*, 446.
(11) Dobson, A.; Robinson, S. D. *Inorg. Chem.* **1977**, *16*, 1321.

(12) The presence of this complex was clearly indicated by mass spectroscopy: *m/e* 590 (P^+).

Table I. Crystal Data for $Mo_2(O_2CCF_3)_4 \cdot 2P(C_4H_9)_3$

mol formula	$C_{32}H_{54}F_{12}O_8P_2Mo_2$
color	orange
cryst dimens, mm	0.19 × 0.18 × 0.19
space group	*I2/a*
cell dimens[a]	
a, Å	19.390 (10)
b, Å	10.414 (4)
c, Å	21.790 (11)
β, deg	94.64 (4)
molecules/cell	4
cell vol, Å^3	4385.58
d_{calcd}, g cm^{-3}	1.586
wavelength, Å	0.710 69
mol wt	1048.59
linear abs coeff, cm^{-1}	6.84
diffractometer	Syntex $P2_1$
mode	θ–2θ
2θ range, deg	6–45
quadrants collected	$+h,+k,\pm l$
no. of data with $F_o > 3\sigma(F_o)$	2593
no. of unique data	2886
total data collected	2980
no. of parameters refined	263
final residuals[b]	
R_F	0.047
R_{wF}	0.064
max Δ/σ, last cycle	0.94

[a] At −125 °C. [b] The function minimized was $\sum w(|F_o| - |F_c|)^2$. The unweighted and weighted residuals were defined as $R_F = (\sum||F_o| - |F_c||)/\sum|F_o|$ and $R_{wF} = \sum w^{1/2}(|F_o| - |F_c|)/\sum w^{1/2}|F_o|$.

Table II. Final Atomic Coordinates (×10^4) for $Mo_2(O_2CCF_3)_4 \cdot 2P(C_4H_9)_3$

atom	*x*	*y*	*z*
Mo(1)	2312.7 (2)	1819.3 (5)	2170.6 (2)
P(2)	1333 (1)	3163 (1)	1660 (1)
O(3)	1681 (2)	952 (4)	2799 (2)
O(4)	2076 (2)	2405 (4)	3488 (2)
C(5)	1726 (3)	1437 (6)	3325 (3)
C(6)	1315 (3)	791 (6)	3812 (3)
F(7)	1734 (3)	387 (7)	4271 (2)
F(8)	954 (3)	−168 (6)	3610 (2)
F(9)	906 (4)	1577 (5)	4066 (3)
O(10)	2960 (2)	145 (4)	2237 (2)
O(11)	2178 (3)	−557 (5)	1502 (2)
C(12)	2708 (4)	−645 (6)	1837 (3)
C(13)	3141 (5)	−1900 (7)	1806 (4)
F(14)	3223 (4)	−2467 (5)	2384 (3)
F(15)	2859 (4)	−2746 (6)	1469 (5)
F(16)	3765 (3)	−1689 (4)	1689 (3)
C(17)	890 (3)	2097 (7)	1088 (3)
C(18)	1340 (4)	1667 (6)	594 (3)
C(19)	968 (4)	738 (7)	134 (3)
C(20)	1425 (5)	338 (8)	−365 (4)
C(21)	655 (3)	3896 (7)	2077 (3)
C(22)	401 (4)	3225 (7)	2609 (4)
C(23)	−209 (4)	3929 (8)	2876 (3)
C(24)	−459 (5)	3313 (10)	3428 (4)
C(25)	1610 (3)	4536 (6)	1217 (3)
C(26)	1062 (4)	5159 (6)	785 (3)
C(27)	1336 (4)	6321 (7)	447 (3)
C(28)	762 (5)	6876 (7)	11 (4)

virtually identical,[13] the equatorial M–P bonds are clearly stronger in the tungsten adduct.[14] Furthermore, a difference of 0.053 (4) Å in the M–P bond lengths could easily translate into a 100-fold increase in the rate of phosphine dissociation[16] (W → Mo) and account for the solution NMR behavior of the alkylphosphine adducts of $Mo_2(TFA)_4$ relative to their tungsten homologues.

Phosphine-Exchange Reactions. An attempt was made to quantify the phosphine-exchange rates of **1c** and $W_2(TFA)_4 \cdot 2PBu_3$

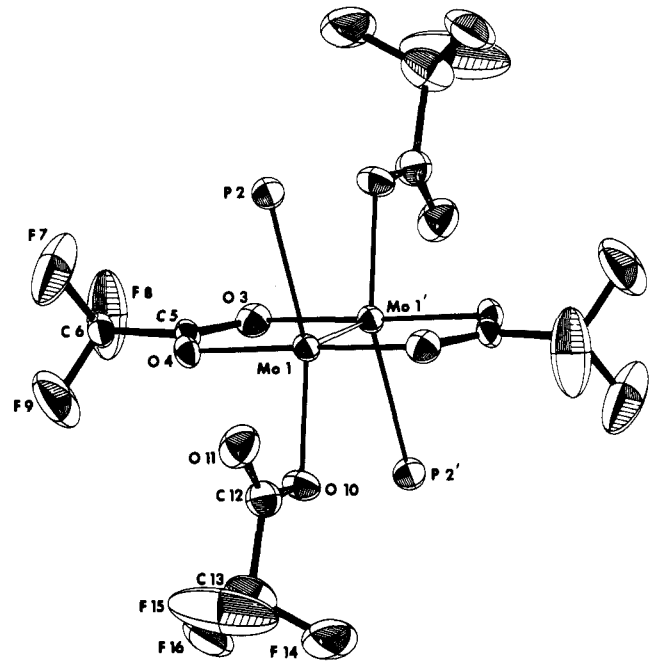

Figure 2. ORTEP drawing of $Mo_2(TFA)_4 \cdot 2PBu_3$ with the *n*-butyl groups deleted. Each atom is represented by a thermal ellipsoid enclosing 50% of its electron density. The molecule resides on a center of symmetry.

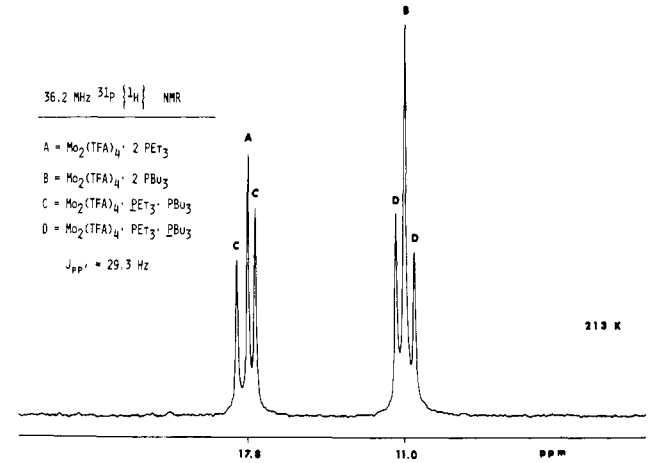

Figure 3. $^{31}P\{^1H\}$ NMR spectrum of an approximately 1:1 mixture of $Mo_2(TFA)_4 \cdot 2PEt_3$ and $Mo_2(TFA)_4 \cdot 2PBu_3$ in toluene-d_8 at −70 °C. See text for discussion.

Table IV. Comparison of Key Bond Lengths (Å) and Angles (deg) in $M_2(TFA)_4 \cdot 2PBu_3$ Complexes

bond length or angle[a]	$Mo_2(TFA)_4 \cdot 2PBu_3$	$W_2(TFA)_4 \cdot 2PBu_3$
M′–M	2.105 (1)	2.224 (1)
M–P	2.542 (2)	2.489 (3)
M–O(3)/O(4) (av)	2.105 (5)	2.107 (8)
M–O(10)	2.146 (4)	2.132 (7)
M–O(11)	2.873 (7)	2.845 (8)
M′–M–P	97.6 (1)	95.7 (1)
M′–M–O(3)/O(4) (av)	91.6 (3)	90.5 (3)
M′–M–O(10)	109.5 (2)	113.0 (2)
M′–M–O(11)	159.7 (2)	161.3 (2)

[a] See Figure 2 for numbering scheme.

(13) Cotton, F. A.; Wilkinson, G. "Advanced Inorganic Chemistry", 4th ed.; Wiley: New York, 1980; pp 822–823.
(14) The contraction *and* strengthening of M–P bonds, as one goes from molybdenum to tungsten, is most likely a relativistic effect,[15] and there is no need to invoke increased M→P dπ–dπ bonding to explain the difference in M–P bond lengths.
(15) (a) Pyykkö, P.; Desclaux, J.-P. *Acc. Chem. Res.* **1979**, *12*, 276. (b) Pyykkö, P.; Desclaux, J.-P. *Chem. Phys.* **1978**, *34*, 261.
(16) Girolami, G. S.; Mainz, V. V.; Andersen, R. A. *J. Am. Chem. Soc.* **1982**, *104*, 2041.

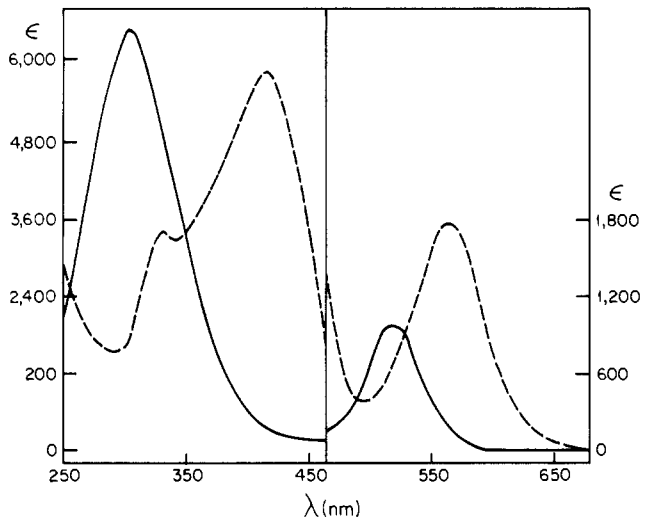

Figure 4. Solution (THF) electronic absorption spectra of $Mo_2(TFA)_4 \cdot 2PMe_3$ (—) and $W_2(TFA)_4 \cdot 2PMe_3$ (- - -).

with PEt_3 under pseudo-first-order conditions, but the rates were too rapid to be followed conveniently by low-temperature $^{31}P\{^1H\}$ NMR spectroscopy. Kinetic studies on two related C_{2h} systems, $Mo_2(O_2C\text{-}t\text{-}Bu)_2X_2(PMe_2Et)_2$ where X = $OSiMe_3$, CH_2SiMe_3, have established that exchange with PMe_3 is a stepwise process and occurs via a dissociative mechanism.[16,17] In order to test for the latter with our complexes, the following experiment was performed. Toluene-d_8 was condensed, at −196 °C, atop an approximately equimolar mixture of **1b** and **1c** in a 10-mm NMR tube. The tube was flame sealed and warmed to −80 °C in the probe of the NMR spectrometer. The $^{31}P\{^1H\}$ NMR spectrum of the mixture is shown in Figure 3. The signals labeled A and B are due to **1b** and **1c**, respectively. The remaining signals (C and D) arise from $Mo_2(TFA)_4 \cdot PEt_3 \cdot PBu_3$, an AB spin system. Each phosphine resonance is split into a doublet of separation $^3J_{PP'}$ (29.3 Hz). A similar experiment was performed with use of $W_2(TFA)_4 \cdot 2PEt_3$ and $W_2(TFA)_4 \cdot 2PBu_3$. In this case, equilibrium (reaction 5) was reached slowly (ca. 30 min) at −80 °C and rapidly

$$Mo_2(TFA)_4 \cdot 2PEt_3 + Mo_2(TFA)_4 \cdot 2PBu_3 \xrightleftharpoons{PhCH_3} 2Mo_2(TFA)_4 \cdot PEt_3 \cdot PBu_3 \quad (5)$$

at −50 °C. The value of $^3J_{PP'}$ for $W_2(TFA)_4 \cdot PEt_3 \cdot PBu_3$ was 27.0 Hz, which is close to the three-bond P–P coupling constant (~31 Hz) obtained from an analysis of the tungsten-183 satellite patterns in the $^{31}P\{^1H\}$ NMR spectra of the individual bisadducts.[6]

We want to mention one other experiment that nicely complements the structural data on the $Mo_2(TFA)_4 \cdot 2PBu_3$ complexes. Toluene-d_8 was condensed, at −196 °C, atop an equimolar mixture of $Mo_2(TFA)_4 \cdot 2PBu_3$ and $W_2(TFA)_4$. The sample was then warmed to −80 °C in the NMR spectrometer, and the ^{19}F and $^{31}P\{^1H\}$ NMR spectra were recorded. The only signals visible were those due to $Mo_2(TFA)_4$ and $W_2(TFA)_4 \cdot 2PBu_3$, i.e., the transfer of phosphine ligands from molybdenum to tungsten was rapid *and* quantitative (reaction 6).

$$Mo_2(TFA)_4 \cdot 2PBu_3 + W_2(TFA)_4 \xrightarrow[-80\ °C]{PhCH_3} Mo_2(TFA)_4 + W_2(TFA)_4 \cdot 2PBu_3 \quad (6)$$

Electronic Absorption Spectra. The most interesting feature of the electronic absorption spectra of quadruply metal–metal-bonded complexes is the $\delta \rightarrow \delta^*$, $^1A_{1g} \rightarrow {}^1A_{2u}$ transition.[18-20] This

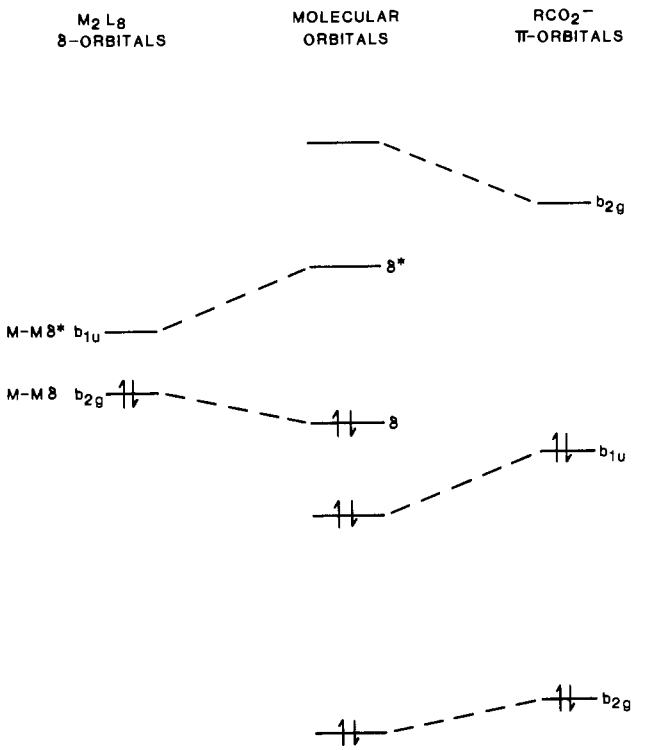

Figure 5. Qualitative energy level diagram showing how the carboxylate π orbitals affect the δ–δ^* separation.

transition occurs at 435 nm (22 990 cm^{-1}) in the solution (THF) spectrum of $Mo(TFA)_4$.[1,21] In Figure 4, we show the solution (THF) absorption spectra of $Mo_2(TFA)_4 \cdot 2PMe_3$ and $W_2(TFA)_4 \cdot 2PMe_3$. The former was recorded at −40 °C,[22] and the extinction coefficients (ϵ) are corrected for an approximately 10% solvent contraction at this temperature; the spectrum of the tungsten complex was recorded at 25 °C. The bands at 519 nm (19 270 cm^{-1}) in the molybdenum spectrum and at 562 nm (17 790 cm^{-1}) in the tungsten spectrum are assigned as the $\delta \rightarrow \delta^*$, $^1A_g \rightarrow {}^1B_u$ transitions (C_{2h} symmetry).

When we compare the solution absorption spectra of $Mo_2(TFA)_4$[1] and $Mo_2(TFA)_4 \cdot 2PMe_3$, we note that the $\delta \rightarrow \delta^*$ transition shifts from 22 900 cm^{-1} in the parent complex to 19 270 cm^{-1} in the trimethylphosphine adduct (ΔE = 3630 cm^{-1}) and it increases in intensity: ϵ = 175 M^{-1} cm^{-1} for $Mo_2(TFA)_4$ and ϵ = 890 M^{-1} cm^{-1} for $Mo_2(TFA)_4 \cdot 2PMe_3$. The low intensities of $\delta \rightarrow \delta^*$ transitions are, as discussed by Trogler and Gray,[18] a consequence of poor orbital overlap, and Mulliken[23] has shown that the oscillator strength of a transition of this type is approximately proportional to the square of the overlap integral. Going from $Mo_2(TFA)_4$ to $Mo_2(TFA)_4 \cdot 2PMe_3$, we expect the effective charge on the metals to decrease in response to the presence of two good σ donors. This leads to an expansion of the molybdenum 4d orbitals, an increase in the δ overlap, and a corresponding increase in the intensity of the $\delta \rightarrow \delta^*$ absorption band. Normally, for a bonding-to-antibonding type transition one argues that increased overlap should blue shift the absorption band.[24] In order to understand the red shift in the present comparison, we have to recognize that the M–M δ and δ^* levels in these complexes have appreciable carboxylate ligand character. In a D_{4h}, $Mo_2(O_2CR)_4$ complex, symmetry-adapted linear com-

(17) The "trick" of using smaller phosphines to slow down the rates of phosphine *exchange*[16] cannot be used here because small phosphines provide equatorial tris(phosphine) adducts, e.g., $M_2(TFA)_4 \cdot 3PMe_3$,[3,6] when excess ligand is present.
(18) Trogler, W. C.; Gray, H. B. *Acc. Chem. Res.* **1978**, *11*, 232.
(19) Cotton, F. A.; Walton, R. A. "Multiple Bonds Between Metal Atoms"; Wiley: New York, 1982; pp 390–413.
(20) Wambaugh, J. "The Delta Star"; Morrow: New York, 1983.
(21) A detailed discussion of the data that led to this assignment can be found in the paper by Martin and co-workers. See: Martin, D. S.; Newman, R. A.; Fanwick, P. E. *Inorg. Chem.* **1979**, *18*, 2511.
(22) At this temperature the equilibrium $Mo_2(TFA)_4 \cdot 2PMe_3 \rightleftharpoons Mo_2(TFA)_4 + 2PMe_3$ lies far to the left, as determined by $^{31}P\{^1H\}$ and ^{19}F NMR spectroscopy.
(23) Mulliken, R. S. *J. Chem. Phys.* **1939**, *7*, 20.
(24) See for example: Sattelberger, A. P.; Fackler, J. P., Jr. *J. Am. Chem. Soc.* **1977**, *99*, 1258.

binations (SALCs) of the filled b_1 and vacant b_1^* π orbitals of the four RCO_2^- ligands span b_{2g} symmetry. In addition, there is a SALC of the filled nonbonding carboxylate a_2 orbitals that spans b_{1u} symmetry. The metal b_{2g} δ and b_{1u} δ^* levels, and the separation between them, are necessarily affected by the presence of ligand π orbitals. In Figure 5, we have drawn a simplified MO diagram to show the effect these ligand π orbitals have on the δ–δ^* separation. The left-hand side of the diagram corresponds to the case where the ligands are pure σ donors. Here the δ and δ^* orbitals are 100% metal in character because there are no ligand SALCs that span b_{2g} or b_{1u} symmetry. A priori, it would be difficult to assess the net effect of the two b_{2g} ligand orbitals on the metal δ orbitals but the SCF–Xα–SW calculations of Norman et al.[25] on HCO_2^- and $Mo_2(O_2CH)_4$ clearly indicate that the interaction of the metal δ level with the higher b_{2g} ligand orbital is the dominant one. This interaction stabilizes the δ level. The situation with regard to the δ^* orbital is straightforward. Relative to the σ-bonding-only case, the δ^* orbital is destabilized by the presence of the ligand b_{1u} orbital. On the basis of these considerations, it is reasonable to conclude that a dimer containing both σ donors and carboxylate ligands should have a smaller δ–δ^* separation and a lower $\delta \rightarrow \delta^*$ transition energy than the parent $M_2(O_2CR)_4$ complex.[26] This conclusion has important ramifications vis-â-vis the electronic absorption spectra of $W_2(O_2CR)_4$ (R = alkyl) complexes. In a recent paper,[1] we suggested that the $\delta \rightarrow \delta^*$ transitions of these tungsten(II) dimers were masked by the intense $\delta \rightarrow \pi^*(OCO)$, $^1A_{1g} \rightarrow {}^1E_u$ absorption bands. If we assume that the $\delta \rightarrow \delta^*$ transition of $W_2(TFA)_4{\cdot}2PMe_3$ has red shifted by ca. 4000 cm^{-1} from its position in the $W_2(TFA)_4$ spectrum, this places the $\delta \rightarrow \delta^*$, $^1A_{1g} \rightarrow {}^1A_{2u}$ transition of $W_2(TFA)_4$ at ca. 460 nm, i.e., *in a region of the spectrum where it would not be visible.*

Summary. We have shown here that $Mo_2(TFA)_4$ forms *isomerically pure* equatorial adducts, $Mo_2(TFA)_4{\cdot}2PR_3$, with trimethyl-, triethyl-, and tri-*n*-butylphosphine. Although the spectroscopic data do not permit an unequivocal assignment of solution stereochemistry, it seems quite reasonable that a C_{2h} core structure, found in the solid state for the PBu_3 derivative, is maintained in solution for all three adducts. We have also demonstrated that the differences in solution behavior between $Mo_2(TFA)_4{\cdot}2PR_3$ and $W_2(TFA)_4{\cdot}2PR_3$ complexes arise from differences in M–P bond strengths: W–P > Mo–P. Finally, we have shown that the lability of phosphine ligands in $M_2(TFA)_4{\cdot}2PR_3$ complexes can be utilized in the synthesis of mixed-phosphine equatorial adducts.

Experimental Section

Reagents. Tri-*n*-butylphosphine (Orgmet), triethylphosphine (Orgmet), and trifluoroacetic acid (Aldrich) were used without further purification. Trimethylphosphine was prepared by a modification[27] of the method of Wolfsberger and Schmidbaur.[28] Sodium trifluoroacetate was synthesized from freshly prepared sodium methoxide and trifluoroacetic acid in methanol. The solid obtained after solvent removal was washed with ether, dried by azeotropic distillation with benzene, filtered, washed with ether, and dried in vacuo (10^{-5} torr, 25 °C, 48 h). Molybdenum trichloride was prepared by the method of Chisholm, Haitko, and Murillo.[29] $W_2(TFA)_4$,[8] $W_2(TFA)_4{\cdot}2PEt_3$,[6] and $W_2(TFA)_4{\cdot}2PBu_3$[6] were synthesized and purified as described earlier. All solvents were purified and dried with use of standard techniques and stored in the drybox.

Physical and Analytical Measurements. Elemental analyses were performed by Schwarzkopf Microanalytical Laboratory, Woodside, NY. Infrared spectra were obtained from Nujol mulls between KBr plates with a Perkin-Elmer Model 1330 infrared spectrophotometer. Samples were prepared in the drybox and run immediately to prevent aerial oxidation.

NMR spectra were obtained on a JEOL FX90Q spectrometer. ^{19}F and ^{31}P NMR spectra were recorded at 84.26 and 36.20 MHz, respectively. Toluene-d_8 and chloroform-*d* were used as internal lock solvents. Chemical shifts (δ) are reported relative to external $CFCl_3$ and 85% aqueous H_3PO_4, both of which are assigned a δ value of 0.0. Negative chemical shifts are assigned to resonances at lower frequency (higher field) than the reference materials.

Mass spectra were obtained on a Finnigan mass spectrometer by the method of direct insertion. Probe temperatures of 30–60 °C and ionizing voltages of 50–70 eV were employed.

General Procedures. All preparations and manipulations were carried out under dry and oxygen-free conditions with use of Schlenk, high-vacuum, or drybox techniques. Our drybox is a Vacuum Atmospheres HE43-2 equipped with a high-capacity purification train (MO-40V) and a Dri-Cold freezer operating at −40 °C.

$Mo_2(O_2CCF_3)_4$. Inside the drybox, a 250-mL Erlenmeyer flask was charged with 150 mL of cold (0 °C) THF, 10 g (49 mmol) of $MoCl_3$, 17.5 mL of 0.5 wt % Na/Hg (51 mmol of Na), 13.6 g (100 mmol) of powdered sodium trifluoroacetate, and a large magnetic stir bar. The flask was stoppered and the mixture was stirred vigorously for 5 h. The dark yellow-brown suspension was then decanted from the mercury and filtered through a 1-in. layer of Celite on a 60-mL medium-porosity sintered-glass frit. The flask was rinsed (2 × 25 mL) with fresh THF, and the combined filtrate and washings were taken to dryness in vacuo. The light brown solid was scraped from the flask, placed in a sublimator, and covered with a thin layer of glass wool. Bright yellow $Mo_2(O_2CCF_3)_4$ sublimed (10^{-5} torr, 100 °C) onto the water-cooled cold finger over the course of several hours. The yield was 3.1 g or 19% based on $MoCl_3$. Anal. Calcd for $C_8F_{12}Mo_2O_8$: C, 14.92; H, 0.00. Found: C, 14.95; H, 0.00. ^{19}F NMR (ppm, toluene-d_8, 84.26 MHz): −72.1 (s). IR (cm^{-1}, Nujol): 1595 ($\nu_{asym}(CO_2)$). Mass spectrum (70 eV): *m/e* 644 (P^+, $^{96}Mo_2(O_2CCF_3)_4$).

$Mo_2(O_2CCF_3)_4{\cdot}2PMe_3$ (1a). Inside the drybox, trimethylphosphine (0.30 mL, 3.0 mmol) was added, via calibrated syringe, to a stirred toluene solution (ca. 15 mL) of freshly sublimed $Mo_2(TFA)_4$ (1.0 g, 1.5 mmol). The bright yellow molybdenum(II) carboxylate solution immediately turned orange, and an orange solid precipitated. After 10 min the suspension was filtered and the orange solid was washed with toluene (3 × 15 mL) and hexane (20 mL) and then dried in vacuo; yield 1.10 g, 90%. The compound was stored at −40 °C inside the drybox. Anal. Calcd for $C_{14}H_{18}F_{12}Mo_2O_8P_2$: C, 21.12; H, 2.28. Found: C, 21.32; H, 2.30. ^{19}F NMR (ppm, THF, −80 °C, 84.26 MHz): −73.9 (s, 1, bidentate $CF_3CO_2^-$), −75.8 (s, 1, monodentate $CF_3CO_2^-$). $^{31}P\{^1H\}$ NMR (ppm, THF, −80 °C, 36.20 MHz): −7.2 (s). IR (cm^{-1}, Nujol): 1665 (s), 1579 (s). Mass spectrum (70 eV): *m/e* 644 ($P - 2PMe_3^+$).

$Mo_2(O_2CCF_3)_4{\cdot}2PEt_3$ (1b). In the drybox, triethylphosphine (0.46 mL, 3.1 mmol) was added, via calibrated syringe, to a stirred toluene solution (ca. 15 mL) of $Mo_2(TFA)_4$ (1.0 g, 1.5 mmol). The solution immediately turned orange, and some orange solid precipitated. At this point the suspension was placed in the freezer (−40 °C) to complete the precipitation. After 4 h, the orange crystalline material was filtered off, washed with cold hexane, and dried in vacuo; yield 1.2 g, 88%. The crystals were stored at −40 °C. ^{19}F NMR (ppm, toluene-d_8, −80 °C, 84.26 MHz): −71.0 (s, 1, bidentate $CF_3CO_2^-$), −74.4 (s, 1, monodentate $CF_3CO_2^-$). $^{31}P\{^1H\}$ NMR (ppm, toluene-d_8, −80 °C, 36.20 MHz): +17.8 (s). IR (cm^{-1}, Nujol): 1667 (s), 1578 (s).

$Mo_2(O_2CCF_3)_4{\cdot}2PBu_3$ (1c). This orange material was prepared in the same manner as **1b**; yield 1.2 g, 75%. The crystals were stored at −40 °C. ^{19}F NMR (ppm, toluene-d_8, −80 °C, 84.26 MHz): −71.3 (s, 1, bidentate $CF_3CO_2^-$), −74.6 (s, 1, monodentate $CF_3CO_2^-$). $^{31}P\{^1H\}$ NMR (ppm, toluene-d_8, −80 °C, 36.20 MHz): +11.0 (s). IR (cm^{-1}, Nujol): 1672 (s), 1585 (s).

X-ray Structure of $Mo_2(TFA)_4{\cdot}2PBu_3$. X-ray quality crystals of **1c** were obtained by slow cooling of concentrated hexane solutions from room temperature to −40 °C. Inside a nitrogen-filled drybag, a well-formed orange block was mounted on a glass fiber with silicon grease and transferred to the liquid-nitrogen-boiloff cooling system (LT-1) of a Syntex $P2_1$ automated diffractometer. From rotation photographs and initial counter data, it was determined that the crystals were isomorphous with the tungsten homologue.[6] Due to the acute β angle, the nonstandard setting $I2/a$[30] was again chosen for data collection. Diffraction data were collected at −124 ± 4 °C. The measured intensities were reduced to structure factor amplitudes and their esd's by correction for background, scan speed, and Lorentz and polarization effects. Corrections for absorption (μ = 6.84 cm^{-1}) or decay were unnecessary. Systematically

(25) Norman, J. G., Jr.; Kolari, H. J.; Gray, H. B.; Trogler, W. C. *Inorg. Chem.* **1977**, *16*, 987.
(26) Similar conclusions have been reached by Manning and Trogler. See: Manning, M. C.; Trogler, W. C. *J. Am. Chem. Soc.* **1983**, *105*, 5311.
(27) Luetkens, M. L., Jr.; Elcesser, W. L.; Huffman, J. C.; Sattelberger, A. P. *Inorg. Chem.* **1984**, *23*, 1718.
(28) Wolfsberger, W.; Schmidbaur, H. *Synth. React. Inorg. Met.-Org. Chem.* **1974**, *4*, 149.
(29) Chisholm, M. H.; Haitko, D. A.; Murillo, C. A. *Inorg. Synth.* **1982**, *21*, 51.

(30) Equivalent positions for $I2/a$ are $^1/_2, ^1/_2, ^1/_2$ and 0, 0, 0 ± *x*, *y*, *z*; $^1/_2 - x, y, -z$.

absent reflections were eliminated, and symmetry-equivalent reflections were averaged to yield a set of unique reflections. Only those data with $F_o > 3\sigma(F_o)$ were used in least-squares refinement.[31]

A Patterson synthesis yielded the positions of the molybdenum atoms. All other non-hydrogen atoms were located with use of successive difference-Fourier syntheses. Positional and thermal parameters (anisotropic for Mo, P, F, O, and C) were refined by full-matrix least squares.[32] Hydrogen atoms were not located and were placed in idealized fixed positions for the final cycles of refinement. Final refinement parameters are given in Table I. A final difference-Fourier map was essentially featureless; the largest peak, 0.97 e Å^{-3}, was located near the CF_3 group of the monodentate carboxylate.

Acknowledgment. We are grateful to the National Science Foundation (CHE-82-06169) for support of this work and the Department of Chemistry, The University of Michigan, for a generous gift of computer time. We also wish to thank Dr. William Butler for his assistance in the X-ray data collection and Professor B. E. Bursten (Ohio State) for helpful discussions on the electronic structure of quadruply metal–metal-bonded complexes.

Registry No. **1a**, 72509-74-1; **1b**, 72509-73-0; **1c**, 98064-56-3; $Mo_2(TFA)_4 \cdot PEt_3 \cdot PBu_3$, 98064-57-4; $Mo_2(TFA)_4$, 36608-07-8; Mo, 7439-98-7.

Supplementary Material Available: Tables of calculated hydrogen atom positions, selected bond distances and angles (Table III), anisotropic thermal parameters, and structure factors for **1c** (9 pages). Ordering information is given on any current masthead page.

(31) All computations were performed with the SHELX-76 program package. See: Sheldrick, G. M. "SHELX-76, Program for Crystal Structure Determination"; Cambridge University: Cambridge, U.K., 1976.

(32) Neutral-atom scattering factors were taken from: "International Tables for X-ray Crystallography"; Kynoch Press: Birmingham, England, 1974; Vol. IV. For hydrogen atoms the values used were those given by: Stewart, R. F.; Davidson, E. R.; Simpson, W. T. *J. Chem. Phys.* **1965**, *42*, 3175.

Contribution from the Department of Chemistry, Georgetown University, Washington, D.C. 20057

Characterization of an Unsymmetrical Oxo–Sulfido Complex, $[(n\text{-Bu})_4N]_2[syn\text{-}(S_2)OMo(\mu\text{-}S)_2MoS(S_2)]$

XINQUAN XIN, NANCY L. MORRIS, GEOFFREY B. JAMESON,* and MICHAEL T. POPE*

Received January 7, 1985

The complex $[(n\text{-Bu})_4N]_2[Mo_2S_7O]$ crystallizes in the orthorhombic space group *Pbca* in a unit cell with dimensions a = 18.026 (3) Å, b = 16.085 (2) Å, c = 31.883 (4) Å, and Z = 8. The structure, described by 396 variable parameters, was refined on F by full-matrix least-squares methods using 2628 reflections with $I > 3\sigma(I)$ in the range 0.0308 Å^{-1} < (sin θ)/λ < 0.4239 Å^{-1} to final values of R and R_w of 0.083 and 0.106. The structure of the $Mo_2S_7O^{2-}$ unit is similar to that of the $Mo_2S_8^{2-}$ anion, except that the apical positions are disordered between O and S. The average Mo–S/O separation of 1.965 (6) Å is in close accord with the electron-weighted average of 1.97 Å from analogous $Mo_2S_8^{2-}$ and $Mo_2S_6O_2^{2-}$ ions. Spectroscopic evidence suggests that the compound is pure and not a solid solution of the above two ions.

Introduction

Molybdenum–sulfur compounds are of importance in the chemistry of several enzymes, such as xanthine oxidase, sulfite oxidase, and aldehyde reductase, and a molybdenum–iron–sulfur cluster is found in nitrogenase.[1] In addition hydrogenation, hydrogendenitrogenation, and hydrodesulfurization are catalyzed heterogeneously by molybdenum–sulfide species.[2] Finally, the study of the condensation of MoS_4^{2-} is an obvious elaboration of the extensive chemistry of polyoxoanions.[3-5] Mononuclear $MoS_nO_{4-n}^{2-}$, n = 0–14, species have been known for some time. Recently, there have been characterized a number of symmetrical di- and trinuclear complexes, such as $Mo_2S_6O_2^{2-}$ and $Mo_2S_8^{2-}$, and one probably unsymmetrical species, $Mo_2OS(\mu\text{-}S_2)(Et\text{-}dtc)_2$ (Et-dtc = *N*,*N*′-diethyldithiocarbamate).[8] We report here the complete characterization of what we believe to be an unsymmetrical compound $[(n\text{-Bu})_4N]_2[(S_2)OMo(\mu\text{-}S)_2MoS(S_2)]$ of the non-carbonaceous molybdenum–sulfur cluster compounds.

Experimental Section

Preparation of the Compound. The title compound was prepared by dissolving 0.65 g of $(NH_4)_2MoS_4$[9-11] in 15 mL of water to which 0.6 mL of 2 N HCl was added with vigorous stirring. The solution turned a dark red color. The complex was crystallized by the addition of 1.8 g of $(n\text{-Bu})_4NBr$ in 10 mL of water (yield 1.3 g) and recrystallized by permitting a hot (60 °C) methanol solution to cool and evaporate over 2 days (yield 0.65 g or 56%) to give dark red daggers with distinctively curved edges, soluble in acetone, acetonitrile, and dimethyl sulfoxide and slightly soluble in methanol. The crystals are weakly deliquescent.

Anal. Found (calcd for $[(n\text{-Bu})_4N]_2[Mo_2S_7O]$): C, 42.38 (41.90); H, 8.28 (7.91); N, 3.12 (3.05); S, 24.96 (24.47); Mo, 21.30 (20.92); O, 1.56 (1.74).

UV–visible spectrum ($(n\text{-Bu})_4N^+$ salt dissolved in CH_3CN): 273 nm (ϵ 1.51 × 10^4 cm^{-1} M^{-1}), 233 nm (2.38 × 10^4), shoulder at 305 nm and

(1) (a) Stiefel, E. I.; Newton, W. E.; Watt, G. D.; Hadfield, K. L.; Bulen, W. A. *Adv. Chem. Ser.* **1977**, *162*, 353. (b) Wentworth, R. A. D. *Coord. Chem. Rev.* **1976**, *18*, 1. (c) Rawlings, J.; Shah, V. K.; Chisnell, J. R.; Brill, W. J.; Zimmermann, R.; Münck, E.; Orme-Johnson, W. H. *J. Biol. Chem.* **1978**, *253*, 1001.

(2) Weisser, O.; Landa, S. "Sulfide Catalysts: Their Properties and Applications"; Pergamon Press: Elmsford, NY, 1973.

(3) Wolff, T. E.; Berg, J. M.; Holm, R. H. *Inorg. Chem.* **1981**, *20*, 174.

(4) Halbert, T. R.; Pan, W. H.; Steifel, E. I. *J. Am. Chem. Soc.* **1983**, *105*, 5476.

(5) Pope, M. T. "Heteropoly and Isopoly Oxometalates"; Springer-Verlag: New York, 1983.

(6) Müller, A.; Diemann, E.; Jostes, R.; Bögge, H. *Angew. Chem., Int. Ed. Engl.* **1981**, *20*, 934.

(7) Stiefel, E. I. *Prog. Inorg. Chem.* **1977**, *22*, 1.

(8) Newton, W. E.; McDonald, J. W.; Yamanouchi, K.; Enemark, J. H. *Inorg. Chem.* **1979**, *18*, 1621.

(9) Müller, A.; Sarkar, S.; Bhattacharyya, R. G.; Pohl, S.; Dartmann, M. *Angew. Chem., Int. Ed. Engl.* **1978**, *17*, 535.

(10) Moore, F. W.; Larson, M. L. *Inorg. Chem.* **1967**, *6*, 998.

(11) For comparison with other tetra-*n*-butylammonium salts the $[(n\text{-Bu})_4N]_2MoS_4$ salt was prepared by addition of an $(n\text{-Bu})_4NBr$ solution to an aqueous solution of $(NH_4)_2MoS_4$ without vigorous stirring. Anal. Found (calcd for $C_{32}H_{72}N_2MoS_4$): C, 54.23 (54.20); H, 10.31 (10.23); N, 3.90 (3.95); Mo, 13.43 (13.53); S, 18.23 (18.08). Red needles; λ_{max}(acetonitrile) 467, 326, 244 nm; λ_{max}(water) 467, 317, 242 nm.

0020-1669/85/1324-3482$01.50/0